Chem Biol Drug Des 2012; **80:** 315–327

Research Article

doi: 10.1111/j.1747-0285.2012.01406.x

Molecular Docking and Dynamics Simulation, Receptor-based Hypothesis: Application to Identify Novel Sirtuin 2 Inhibitors

Sugunadevi Sakkiah, Sundarapandian Thangapandian, Chanin Park, Minky Son and Keun W. Lee*

Division of Applied Life Science (BK21 Program), Systems and Synthetic Agrobiotech Center (SSAC), Plant Molecular Biology and Biotechnology Research Center (PMBBRC), Research Institute of Natural Science (RINS), Gyeongsang National University (GNU), 501 Jinju-daero, Gazha-dong, Jinju 660-701, Korea
**Corresponding author: Keun W. Lee, kwlee@gnu.ac.kr*

Sirtuin, NAD$^+$-dependent histone deacetylase enzyme, emerged as a potential therapeutic target, and modulations by small molecules could be effective drugs for various diseases. Owing to the absence of complex structure of sirtuin 2 (SIRT2), sirtinol was docked in the NAD$^+$ binding site and subjected to 5-nseconds molecular dynamics (MD) simulation. LigandScout was used to develop hypotheses based on 3-representative SIRT2 complex structures from MD. Three structure-based hypotheses are generated and merged to form dynamics hypothesis. The dynamics hypothesis was validated using test and decoy sets. The results showed that dynamic hypothesis represents the complementary features of SIRT2 active site. Dynamic hypothesis was used to screen ChemDiv database, and hits were filtered through ADMET, rule of five, and two different molecular docking studies. Finally, 21 molecules were selected as potent leads based on consensus score from LigandFit, Gold fitness score, binding affinity from VINA as well as based on the important interactions with critical residues in SIRT2 active site. Hence, we suggest that the dynamic hypothesis will be reliable in the identification of SIRT2 new lead as well as to reduce time and cost in the drug discovery process.

Key words: cluster analysis, LigandScout, molecular dynamics, sirtuin, structure-based pharmacophore

Received 17 January 2011, revised 5 April 2012 and accepted for publication 24 April 2012

The term 'epigenetic' refers to heritable changes in gene expression that occur without any changes in DNA sequence (1). These heritable changes are achieved by different post-translational histone modifications like arginine and lysine methylation, serine and threonine phosphorylation, ubiquitinylation or lysine acetylation, which all contribute to epigenetic gene regulations (2,3). The sum of all different modifications and their interactions with each other is called the histone code (4,5). The regulation of gene patterns depends on the acetylation and deacetylation balance process of chromatin. Deacetylation is one of the post-translational modifications by histone deacetylases (HDACs). HDACs deacetylate the α-amino group of lysine residues in histone tails and also many other nonhistone proteins, such as p53, FOXO, tubulin, and BCL6. Histone acetyltransferases possess an opposing activity for HDACs, which transfer the acetyl groups to lysine residues. Both ensure a balance between acetylation and deacetylation of chromatin, and a shift in this balance results in changes in gene regulation (6). Eighteen HDAC enzymes have been identified and classified into four groups based on its sequence homology (7,8). Class I (HDAC1, 2, 3, and 8), Class II (HDAC4, 5, 6, 7, 9, and 10), and Class IV (HDAC 11) are related to the RPD 3/HDA1 deacetylase family (9). Class III enzymes, sirtuins, require nicotinamide adenine dinucleotide (NAD$^+$) as a cofactor for their catalysis process (10). Until now, seven different members (SIRT1–7) of NAD$^+$-dependent HDACs have been discovered in humans (11,12), and together, they show homology to the yeast protein Sir2. Sirtuins are connected to several cellular processes in prokaryotic, archae, and eukaryotic cells (13–16). Among seven mammalian sirtuins, we select SIRT2 as our target because of the following reasons.

Structural Details of Sirtuin 2

Human sirtuin type 2 (SIRT2) is predominantly a cytoplasmic protein except in G2/M transition and in mitosis (17). SIRT2 has a catalytic core with two distinct domains: (i) small domain consists of helical domain containing a pocket lined with solvent-exposed hydrophobic residues and zinc-binding domain, zinc ion tetrahedrally co-ordinated with four cysteine residues, and (ii) larger domain is a variant of the Rossmann fold (18). A large groove is formed at the interface of these two domains, and it will be a recognized portions for substrate as well as for a class-specific protein-binding site (19). The catalytic domain catalyzes a two-step reaction that requires NAD$^+$ as a cosubstrate. The first series of reactions is the cleavage of the nicotinamide-ribose glycosidic bond of NAD$^+$, which results in the release of a free nicotinamide and in the formation of a relatively long-lived peptidyl imidate intermediate (20). Second is the transfer of acetyl group to ADP-ribose with the production of *O*-acetyl-ADP-ribose (21,22).

Importance of Sirtuin 2

SIRT2 could be a potential therapeutic target for the treatment of cancers (23,24) or the modification of physiological processes that may involved in calorie restriction such as the aging process (15), fat storage (25,26), neurodegeneration (27), diabetes, and heart failure (28). α-Tubulin is one of the substrate for SIRT2 that deacetylases the acetylated Lys40 and co-localizes with cytoplasmic microtubules together with HDAC6 (29,30). The acetylation status of microtubulin network is formed from α- and β-tubulin heterodimers that play a crucial role in the regulation of cell shape, intracellular transport, cell mobility, and cell division (31). Recent studies have provided strong evidences that the biological function of SIRT2 can be linked to tumorigenesis and in the development of Parkinson's disease (32,33). Many studies have reported that SIRT2 participates in the cell cycle in several types of cells. Understanding the involvement of SIRT2 in cell cycle regulation can lead to the new therapeutic possibilities. The study in glioma cell lines provided evidence that SIRT2 may function as a novel checkpoint enzyme in early metaphase (M) to prevent chromosomal instability (34). SIRT2 phosphorylation and increase during G2 and M phases and play a role in the control of G2 to M transition (35). It was recently reported that SIRT2 decreases the transcriptional activity of P53 through the interaction with 14-3-3 β and γ proteins. In addition, SIRT2 has also been reported to interact with several transcription factors Hoxa10, FoxO1, and FoxO3a (36,37). SIRT2 has been connected to cell death in response to various stress stimuli including DNA damage (38). Moreover, it has been suggested that sirtuin cannot be compensated by Classes I-II and IV HDACs. Hence, designing potent sirtuin inhibitor could increase their overall chemotherapeutic efficacy (39,40); therefore, there has been an increasing interest in the development of sirtuin inhibitors (41).

Strategy to Find the Novel Inhibitors for Sirtuin 2

The computational techniques help in drug design process to dramatically widen the chemical space and reduce the number of candidates for experimental validation (42). Pharmacophore modeling and virtual screening is an inexpensive and fast alternative powerful tool to identify the potential lead for various targets. Because of the absence of complex SIRT2 structures in protein data bank, molecular docking study was carried out. *LigandFit* from DISCOVERY STUDIO v2.5 (DS, http://www.accelrys.com) was used to dock the sirtinol in the NAD^+ binding site of SIRT2 and to validate it based on its critical hydrogen bond reported in the literatures (43,44). The best complex from LigandFit was subjected into 5-ns molecular dynamics (MD) simulation using GROMACS (45–47) to confirm the ligand stability in NAD^+ binding site. Three representative structures were selected to generate the structure-based hypothesis based on cluster analysis implemented in GROMACS. LigandScout (48,49) was used to generate the structure-based hypothesis (three representative structures), and the dynamic hypothesis was generated by superimposing the three structure-based hypotheses and the removing the overlapped chemical features. The dynamics hypothesis was validated using test and decoy set to find how well it can differentiate the active from inactive inhibitors. The dynamics hypothesis was used as a query in virtual screening of CHEMDIV database (www.chemdiv.com, ChemDiv, Inc., San Diego, CA, USA). The hits are sorted out by applying several filters, such as Lipinski's rule of five, ADMET properties, and subsequently subjected to molecular docking process. The molecular docking studies were performed using *LigandFit* and *Genetic Optimization for Ligand Docking* (*GOLD*, Cambridge Crystallographic Data Center) to find the suitable orientation of leads in the active site of SIRT2 (50).

Methods and Materials

Molecular docking protocol to prepare sirtuin2 complex

Information on the interaction properties of substrate/inhibitors is required to efficiently design the new inhibitors. In the absence of SIRT2 complex structure, sirtinol, one of the potent inhibitors for sirtuin family, was selected to produce the complex structure using molecular docking study. Hence to produce a SIRT2 complex, apoform of SIRT2 (PDB: 1J8F, resolution 1.70 Å) was used as a receptor and the hanging N-terminal helix (G34-F45) was removed. *LigandFit* module (51) from DS was utilized to dock the sirtinol in SIRT2 active site. Before initiating the docking study, the receptor was neutralized by removing the water molecules and hydrogen atoms were added by applying CHARMm force field (52). The added hydrogen atoms were attained its suitable orientation in receptor by applying position restrained energy minimization. The 2D format of sirtinol was drawn using ChemSketch and converted into 3D format by exporting into DS. To obtain the most stable energy-minimized conformation of these molecules, maximum number of 25 conformations were generated for each by applying Poling algorithm (53) using the *Best Conformation* module with a constraint of energy value >20 kcal/mol from the global minimum.

After the protein preparation, the suitable binding site for sirtinol was identified before initiating the docking process. The active site of protein was represented as binding site and identified using two methods: firstly, based on the shape of receptor using 'eraser' algorithm and secondly, volume occupied by the known ligand poses already in an active site. In our case, eraser algorithm was applied to detect the suitable binding pocket for sirtinol. To confirm the binding orientation of sirtinol in SIRT2, sir2Af2 sirtuin (PDB ID: 1YC2) (51) was used as a reference structure. The docking process saved top 10 conformations for each molecule based on dock score after the energy minimization using the smart minimizer method which begins with steepest descent algorithm and followed by conjugate gradient method.

Molecular dynamics simulation

The selected complex from docking study and apo-form of SIRT2 (PDB ID: 1J8F) were subjected to 5 nseconds of MD simulations using GROMACS 3.3.0 (http://gromacs.org) software package (47) in which a leap-frog integration step was applied to solve the equations of motion. The GROMOS96 (45) force field was utilized to simulate the complex structure that was employed to observe the ligand sustainability in NAD^+ binding pocket and to permit the flexible interactions. Special bond was used to place a Zn in its original place (anchored between the four conserved

cysteine residues) throughout the MD simulation The molecular topology file for sirtinol was constructed by submitting into PRODRG (54) web server (http://davapc1.bioch.dundee.ac.uk/programs/prodrg), and no new atom types are included so that the atom charges and force constants defined in the GROMOS96 force field remained constant. A cubic box of 1 nm as a minimum distance between protein and box edges was generated to solvate the systems. The SPC (55) water model was used to create aqueous environment, and periodic boundary conditions were applied in all directions. To neutralize the systems, two and four Na^+ ions are used to replace the water molecules present in apo and complex systems, respectively. A twin range cut-off was used for long-range interactions: 0.8 nm for van der Waals interactions and 1.4 nm for electrostatic interactions. LINCS (56) and SETTLE (57) algorithms are used to constrain all bond length and to constrain the geometry of water molecules, respectively. Steepest descent algorithm was utilized for energy minimization with a tolerance of 2000 kj/mol/nm to relieve the unfavorable contacts of system and subjected to 50 pseconds equilibration run. Afterward, this pre-equilibrated system was used for 5 nseconds of MD simulation with a time step of 2 fseconds at constant temperature (300 K), pressure (1 atm) (58). Subsequently, to relax the solvent molecules present in the systems, 100 pseconds of position restrained and conformations were collected at every 5 pseconds and analyzed using GROMACS analysis tools. The results were analyzed by Cluster analysis provided by the GROMACS package to select the representative structures and refined by applying the steepest descent followed by conjugate gradient energy minimization which was used to develop the dynamics structure–based pharmacophore model.

Selection of an ensemble of representative snapshots

The 5 nseconds of MD simulations trajectory was used to select a few representative snapshots that represent the conformational flexibility of protein. The trajectory structures can be clustered by applying several methods such as Jarvis Patrick, single linkage, Monte Carlo diagonalization, Gromos. We mainly focused on single linkage algorithm, for cluster analysis, which adds a structure into a cluster when the distance to any element of cluster is less than cut-off of 0.107 nm. First, an XPM matrix file is generated with the RMSD comparison of each snapshot with all the others.

Structure-based pharmacophore generation

Generation of receptor/structure-based pharmacophore models using LigandScout

The interactions between protein and ligand are used as a basic information to construct the receptor-based pharmacophore model. The three representative (SIRT2 complex) structures from MD simulation were used to generate structure-based pharmacophore model. A ligand interaction with critical amino acids present in the active site of protein was a sufficient input to generate the structure-based pharmacophore. Two software tools were used to key out the crucial pharmacophore patterns: (i) LigandScout, used to study the interactions between the inhibitors and the critical amino acids in SIRT2 active site as well as used a tool for automatic construction and visualization of pharmacophore model derived from the 3D co-ordinates of proteins (59). The software extracts and interprets ligand–receptor interactions such as hydrogen bonding, charge transfer, hydrophobic regions of their macromolecular environment from PDB co-ordinates of the complex structures which automatically create and visualize the advanced 3D pharmacophore model. (ii) DS was used for the conversion of .hypoedit to .chm file, which is a suitable format for screening the multiconformational three-dimensional chemical structure databases. The pharmacophore model that complements the receptors' active site residues is developed by considering the receptor–ligand flexibility. Each pharmacophore was developed based on the direction of interactions of inhibitor, and the three structure–based pharmacophore models were merged and the overlaid chemical features are removed to construct a dynamic pharmacophore model.

Validation of dynamics hypothesis

In order to validate the dynamic hypotheses, two kinds of data set were constructed, test and decoy sets. Test set contains 25 diverse compounds with the activity value (IC_{50}) between 0.41 and 136 nM, which were classified into active (IC_{50} < 7 nM = +++), moderate active (7 nM ≤ IC_{50} < 70 nM = ++) and low active (IC_{50} ≥ 70 nM = +) SIRT2 inhibitors. ChemSketch was used to sketch the two-dimensional chemical structures of all compounds and converted into their corresponding 3D format by exported into DS. *Best Conformation* module was used to generate the 255 conformations of each compound to assure the energy-minimized conformation by applying CHARMm (61) force field and Poling algorithm [41]. The conformations with energy value higher than 20 kcal/mol from the global minimum were rejected. The test set was given as input to the *Ligand pharmacophore mapping* protocol to find how well the selected hypothesis was able to predict the external molecules. Test set is mainly used to evaluate how well the dynamic hypothesis distinguished between active and inactive inhibitors.

Decoy set was prepared by calculating the 1D property of 2000 molecules. The main purpose of this validation is to check the predictability of the dynamics hypothesis based on the statistical parameters. The decoy set contains 15 active SIRT2 inhibitors and the remaining unknown or low active SIRT2 inhibitors. GH and EF are the two main factors that can predict the capability of the hypothesis. An GH and EF were calculated using the below formula

$$GH = [(H_a(3A + H_t))/(4H_tA))(1 - ((H_t - H_a)/(D - A))]$$

$$EF = [((H_a/H_t)/(A/D))/100]$$

where H_a = the number of active molecules in the hit list, H_t = the number of hits retrieved, A = the number of active molecules present in the database, and D = the total number of molecules in the database.

Virtual screening

The resultant dynamics pharmacophore model was applied in virtual screening of ChemDiv database to retrieve the hits using *Ligand*

*Pharmacophore Mapping/*DS. The screened molecules were tested for drug-like properties by applying ADMET and Lipinski's rule of 5. In ADMET properties, the BBB, solubility, and absorption criteria were mainly focused; if the molecules have the levels of 3, 3, and 0, it represents that the molecules have good BBB, solubility, and absorption, respectively. According to the rule of 5, compounds are well absorbed when they possess LogP less than 5, molecular weight below than 500, number of HBDs < 5, number of HBAs less than 10, and number of rotatable bonds <10. The compounds that satisfied all the above filtrations were selected for molecular docking studies in order to determine the suitable orientation of leads.

Molecular docking protocol to refine the virtual screening leads

Combining the virtual screening and molecular docking techniques has become one of the reputable methods in drug discovery and enhancing the efficiency in lead optimization. To evaluate the accuracy of docking program, *LigandFit/*DS and *GOLD* were used in this study for the purpose of getting unbiased results. There is no single docking algorithm or scoring function that can correctly predict the binding affinities of ligands in every protein–ligand complex. Hence in this study, two different docking programs (*LigandFit* and *GOLD*) were investigated on the test set molecules as well as on the leads to identify the binding mode of ligands in the active pocket of a protein and to predict the binding affinity between the ligand and protein.

LigandFit/DS

LigandFit was executed for favorable orientation of ligands in protein active site. For docking study, initially receptor was prepared by removing the water molecules and CHARMm force field was applied using *Receptor–Ligand Interaction/*DS. The active site was identified by the volume occupied by sirtinol as well as the critical residues reported in literatures. The database hits and the 20 known SIRT2 inhibitors were docked in the active site of SIRT2. During the docking process, top 10 conformations were generated for each ligand based on the dock score value after the energy minimization using the smart minimizer method, which begins with the steepest descent method followed by conjugate gradient method. Each of the saved conformation was evaluated and ranked using the scoring functions including LigScore1, LigScore2, PLP1, PLP2, JAIN, PMF, and LUDI. The docked poses were validated by the consensus scoring function and hydrogen bond interactions between the candidate molecules and active site residues. All the ligands, which formed the good hydrogen bond interactions with Q167, N168, I169, and D170 as well as hydrophobic interactions, were selected as the potent leads for SIRT2.

GOLD

The binding orientation of compounds retrieved from dynamic pharmacophore model was evaluated using *GOLD* molecular docking program. The *GOLD* program from Cambridge Crystallographic Data Center, UK, uses a genetic algorithm for docking flexible ligands into protein-binding site (50). The ligand molecules were docked within a radius of 10 Å around the carboxyl group of Q167. Docking calculations were made using the default *GOLD* fitness function and default evolutionary parameters: population size = 100; selection pressure = 1.1; # operations = 100,000; # islands = 5; niche size = 2; migration = 10; mutation = 95; cross-over = 95. Ten docking runs were performed per structure unless three of the 10 poses were within 1.5 Å rmsd of each other. All the hit molecules as well as two active compounds were docked into binding site of SIRT2. The interacting ability of a compound mainly depends on the fitness score: greater the *GOLD* fitness score, better the binding affinity. Hit molecules that showed the expected interactions with the critical amino acids present in the active site of protein and comparable high binding scores with the bound ligand were selected as potent inhibitors of SIRT2.

Results and Discussions

Molecular docking study for sirtuin2 complex using LigandFit

Molecular docking approach, one of the reputable methods in drug discovery process, was used to find the solution to disclose the critical residues for ligand binding in protein. *LigandFit/*DS was used to gain the insight into most probable inhibitors' binding conformations in active site of specific protein. Docking accuracy, measured by the relative true binding mode of small molecules in active site of receptors, determines the quality of docking methodology. Molecular docking was carried out using SIRT2 apo-form as a receptor to make visible binding orientation of inhibitor in SIRT2 active site. The suitable orientation of sirtinol was picked out by comparing with SIR2AF2 (PDB ID: 1YC2) crystal structure (60). The docked sirtinol was well placed in the suitable binding pocket and showed all necessary interactions reported in literatures (60,61). The final selected SIRT2 complex was subjected to MD simulation to observe that how well the sirtinol was placed in its original position as well as how well the structure changes owing to inhibitor binding.

Molecular dynamics simulations

The best SIRT2–sirtinol complex from *LigandFit* and apo-form of SIRT2 were subjected to 5-ns MD simulations using GROMACS (45–47). The protein stability for the two systems was confirmed by plotting root mean square deviation (RMSD) and radius of gyration (R_g) of protein. The two-dimensional RMSD plot of Cα atoms was drawn throughout the trajectory by keeping starting structure (t = 0) as a function of time. The RMSD plot of apo-form and complex structure has shown deviation between 0.33 and 0.35 nm (Figure 1). This value indicates that both the systems are well stabilized during our simulation period. To find the flexibility of each residue along the polypeptide chain, which is the Cα atom of a particular residue averaged over the entire simulation time (4), root mean square fluctuation (RMSF) was computed. Results of RMSF showed that the α-helices and β-strands are well stabilized (not shown much deviation) as expected and the peak in two-dimensional plot represents that loop regions are flexible (Figure 2). The averaged structures from last 2 nseconds were used for comparative study as well as to distinguish the transformation between apo-form and complex SIRT2. In sirtuin family, the NAD^+ binding pocket was classified into three sites: A-site: adenine group of NAD^+ interacts with the residues such as

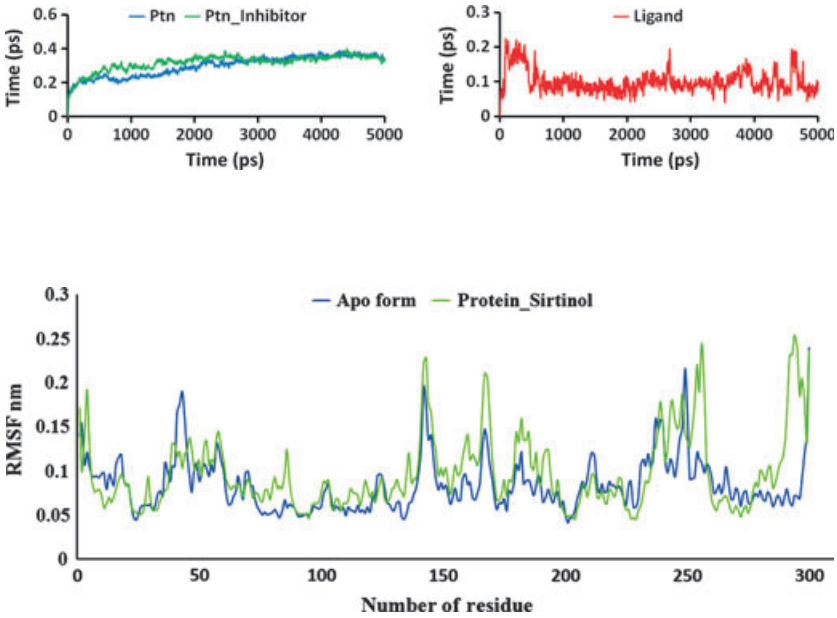

Figure 2: Local conformational changes indicated by atom-positional root mean square fluctuations calculated with respect to the average structure of apo-form, bound with sirtinol derived by molecular dynamics simulations.

N286, E288, G86, G261, C324, K287, E323; B-site: NAD^+ ribose formed an interactions with H187 and Q167; and C-site: nicotinamide part of NAD^+ was placed in a suitable orientation for deacetylation process. S88, N178, H149, D180, I179, F96, and A91 are the crucial residues present in C-site and involved in polarization and hydrolysis of NAD^+ glycosidic bond. It was hypothesized that sirtinol occupied in C-site of NAD^+ binding pocket and reduced the flexibility of F96 residue in Loop3 (Figure 3). Here mainly, we focused on C-site of NAD^+ binding pocket because the inhibitor should occupy this site to change the active SIRT2 to inactive. Hence, the distance between the residues occupied in neck of C-site was computed from initial and representative structures to calculate its size. Apo and complex structures showed a distance of 11.97 and 20.80 Å between the H187 and F96, respectively (Figure 4). From this analysis, we suggest that the increasing distance in complex form distorted the assembly of C-site of NAD^+ binding pocket. The initial complex structure showed a distance of 8.44 Å between phenyl group of F96 (present in Loop3) and sirtinol but the distance was increased to 13 Å in representative complex structure (Figure 5). The flexibility of Loop3 will play a major role in NAD^+ accommodation in SIRT2 active site. The sirtinol moves F96 outside the active site with the support of partial distortion of Helix 3 and the flexibility of Loop3 was hindered. Therefore, we suggest that any small molecules which reduce the flexibility of Loop3 might be a good inhibitor and also it was proved that the sirtinol occupies a perfect place and orientation in SIRT2 during our simulation process. The trajectory was clustered by applying the single linkage method from GROMACS. This method initially generates the XPM matrix based on RMSD, which compares the each snapshot with all the others. Then, it adds the structures into cluster when the distance between the elements of the cluster is less than the cut-off value of 0.107 nm. From the total of ten clusters (Figure 6A), three representative structures (Figure 6B) were selected to generate the structure-based hypothesis (from the top three populated clusters).

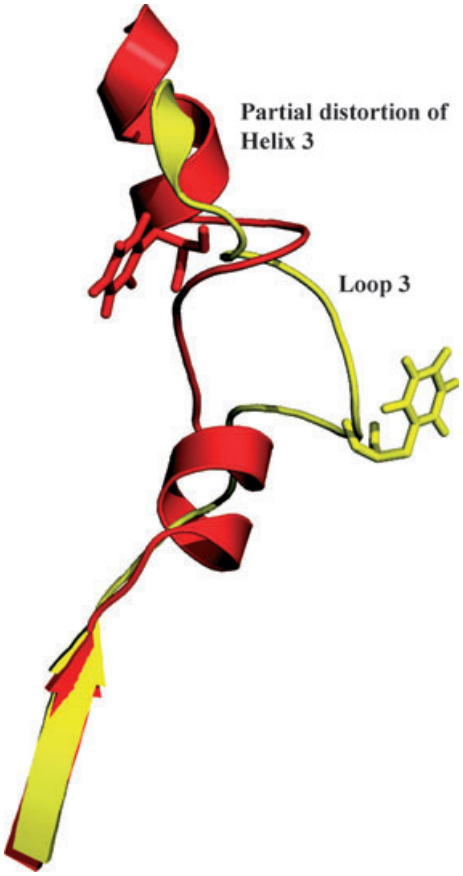

Figure 3: Structural representation of flexibility of Loop3 in SIRT2. apo-form (red) and complex (yellow) indicate that the F96 in Loop3 moves far away from its original position owing to sirtinol binding.

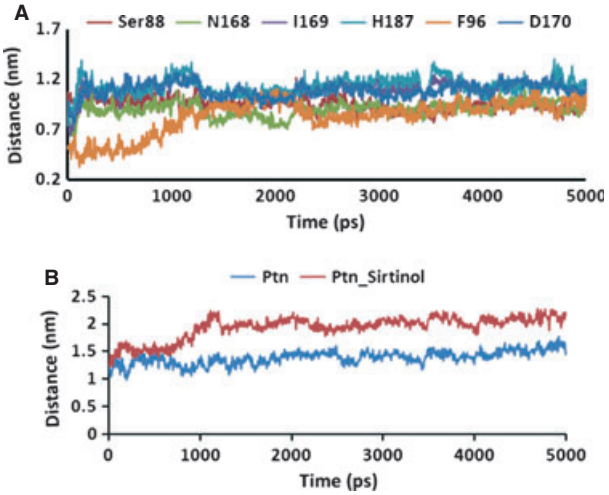

Figure 4: (A) The distance between sirtinol and highly conserved C-site residues (S88, F96, N168, I169, D170, H187) and (B) Time trace of Cα-Cα distance between residues F96 and H187 plotted as a function of time to highlight the difference in the orientation of the conserved F96 in the Loop 3 are plotted throughout the 5-nseconds MD simulation.

Receptor-based pharmacophore model generation

Main aim of this work is to develop a reliable dynamic hypothesis to find suitable small molecules that can inhibit the SIRT2 function. From MD simulations, three representative structures were used to generate the structure-based hypothesis. LigandScout was used to generate the hypothesis based on the ligand–receptor interactions such as hydrogen bonding, charge transfer, and hydrophobic regions from complex structures. Multiple chemical features were detected and mapped onto the ligand functional groups that allow the user to export knowledge on SIRT2 inhibitors. Alternative hydrogen bond acceptor (HBA) and/or hydrogen bond donor (HBD) sites are considered simultaneously on the protein within the limits of geometric constraints. Excluded volume spheres were also added to structure-based hypothesis onto co-ordinates defined by protein side chain atoms to characterize the inaccessible areas for any potential ligand. The 3D co-ordination of the interaction point was obtained from LigandScout and results in specific interaction model that can map the ligands in their bioactive conformation. DS was used for the conversion of LigandScout hypothesis (.hypoedit) to .chm file, which is a suitable format for screening the multiconformational chemical databases. Three hypotheses were generated based on the three representative structures. Hypo1 and Hypo2 are five-feature hypotheses containing similar chemical features (4 hydrophobic (Hy) and 1 HBD) but Hypo3 is a four-feature pharmacophore model comprising only Hy group (Figure 7). The dynamic hypothesis was produced by superimposing the three structure-based hypotheses and removing the overlapped chemical features. Finally, the 6-feature (1 HBD and 5 Hy) dynamics hypothesis was obtained (Figure 7).

Validation of dynamics pharmacophore model

The dynamic pharmacophore model was validated using two different methods: (i) test set, to validate how well the dynamics hypothesis picks the active from inactive compounds, and (ii) decoy set, to evaluate the predictability of the hypothesis using statistical parameters. The test set contains 25 structurally diverse molecules that were classified into three different categories based on its IC_{50} values (explained in Methods and Materials), that is, highly active, moderately active, and low active compounds. High number of chemical features will reduce the hit rates; hence, we set a criteria that any small molecules which satisfied the five chemical features present in the dynamics hypothesis will be a good lead. Dynamic pharmacophore was used as query in Ligand pharmacophore mapping module from DS to screen the test set. The fit value of the screened test set molecules was compared with the known activity value of SIRT2 inhibitors. The result shows that all the active compounds show a fit value of greater than 2.5, moderately active inhibitors have the values between 1 and 2.5, and the low active compounds show a value <0 (Table 1). The test set screening result clearly shows that the dynamic hypothesis can differentiate the active from inactive inhibitors effectively. One of the active and low active compounds fit with the dynamics hypothesis was shown in Figure 8.

Next decoy set was used to determine the predictability of the dynamics hypothesis by calculating various statistical parameters. Decoy set comprises 15 known good inhibitors and 1985 decoy molecules of SIRT2 inhibitors. This validation also revealed how well the dynamics hypothesis can discriminate the active from inactive or unknown compounds. The database screening was performed using *Ligand Pharmacophore Mapping* module. The result was analyzed using a set of parameters such as hit list (H_t), number of active percent of yields (%*Y*), percent ratio of actives in the hit list (%*A*), enrichment factor (EF), false negatives, false positives, and goodness of hit score (GH) (Table 2). Dynamics hypothesis successfully retrieved 86.67% of active compounds from the decoy set. The EF and GH are important statistical parameters to determine the predictability of the hypothesis. In general, the best pharmacophore

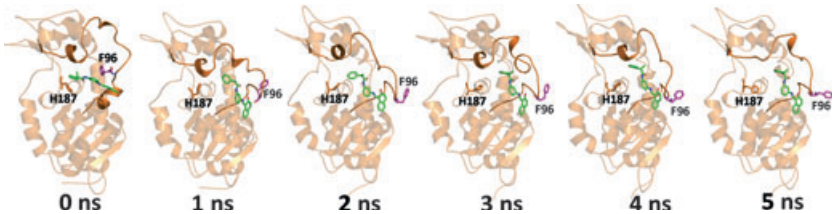

Figure 5: The snapshots at 0, 1, 2, 3, 4, and 5 nseconds MD simulations and the important residues are shown in stick and the inhibitor (Green).

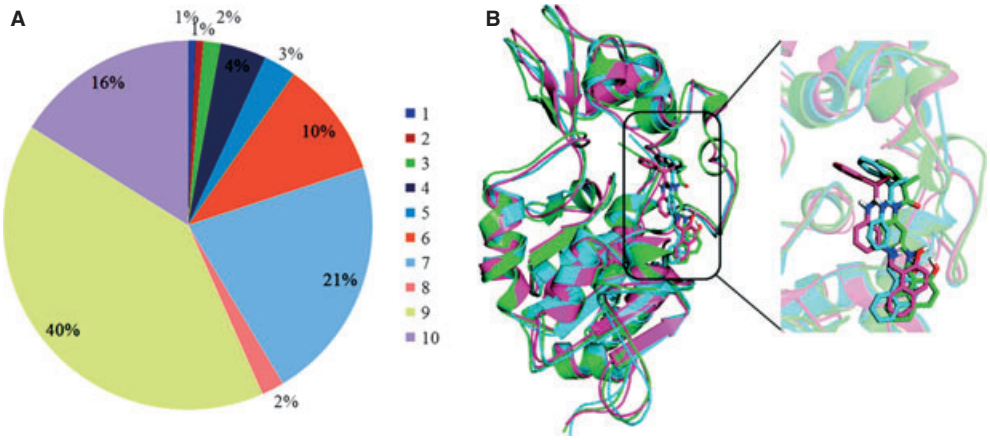

Figure 6: (A) The pie chart obtained from the cluster analysis of 5-nseconds conformational space of SIRT2 with sirtinol shows ten clusters represented by different colors and the percentage of conformers in each cluster (B) The superimposition of three cluster representative structures of cluster 7 (green), cluster 9 (cyan), and cluster 10 (magenta) structures, where Hy (hydrophobic), hydrogen bond donor, and hydrogen bond acceptor are illustrated in blue, magenta, and green, respectively.

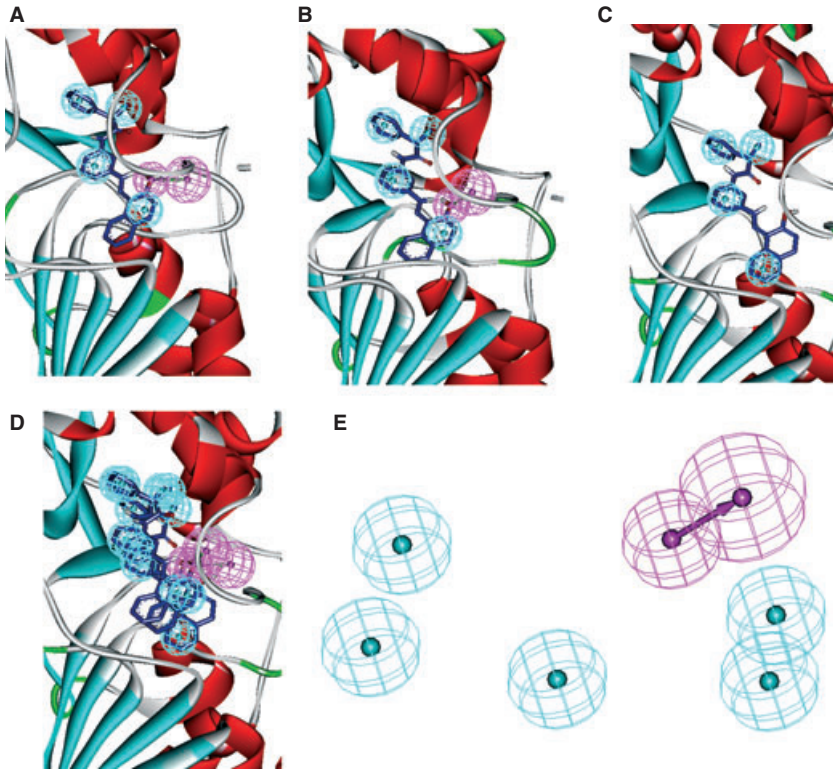

Figure 7: Receptor-based pharmacophore model from the highly populated clusters (A) Cluster 7 (Hypo1), (B) Cluster 9 (Hypo2), (C) Cluster 10 (Hypo3), (D) overlay of all the three structures, (E) dynamics pharmacophore model (the overlapped chemical features are removed). Pharmacophoric features are color-coded, Hydrophobic: Cyan (Hy); Hydrogen bond donor: Magenta (HBD).

model should show the GH score greater than or equal to 0.6 and the EH value close to 1. The dynamic hypothesis shows GH of 0.71 and EF of 0.87, which indicates the good predictability of our hypothesis.

Overall validations confirmed that the dynamics hypothesis can discriminate the active from low active inhibitors. Any small molecules that satisfied the chemical features with their specific constrains in the dynamic pharmacophore can inhibit the SIRT2 activity. Hence,

Table 1: Fit values of each compounds in the test set using dynamic hypothesis

Name	Chemical formula	Activity IC_{50} nM	Fit value	Name	Chemical formula	Activity IC_{50} nM	Fit value
Salermide	$C_{26}H_{22}N_2O_2$	0.41	4.53	Test1	$C_{32}H_{32}F_2N_4O_3$	51	1.29
Suramin	$C_{55}H_{48}N_6O_5$	1.15	4.45	Tripos360702	$C_{32}H_{34}F_2N_4O_3$	51	1.25
67	$C_{57}H_{52}N_6O_5$	1.2	4.32	JFD00244	$C_{30}H_{25}ClN_2O_3$	56.7	1.10
Nf675	$C_{48}H_{43}N_5O_4$	2.26	3.57	Comp48	$C_{21}H_{20}F_3N_5O_2S$	57	1.09
AKG2	$C_{23}H_{13}Cl_2N_3O_2$	3.5	3.06	Cambinol	$C_{21}H_{16}N_2O_2S$	59	1.04
Comp40	$C_{23}H_{14}ClN_3O_2$	5.5	2.96	Test2	$C_{32}H_{34}N_4O_3$	63	1.02
Comp41	$C_{24}H_{14}F_3N_3O_2$	6	2.53	66	$C_{26}H_{22}N_2O_2$	74	0.59
P_sirtinol	$C_{26}H_{22}N_2O_2$	25.9	2.02	CD04097	$C_{21}H_{18}Cl_2N_2O_3S$	74.3	0.40
Test6	$C_{22}H_{23}N_{23}O_3$	47	1.60	Test9	$C_{23}H_{24}FN_3O_3$	80	0.60
R_sirtinol	$C_{26}H_{22}N_2O_2$	49.3	1.59	Test27	$C_{29}H_{33}N_3O_3$	86	0.93
Test5	$C_{23}H_{25}N_3O_3$	56.7	1.10				

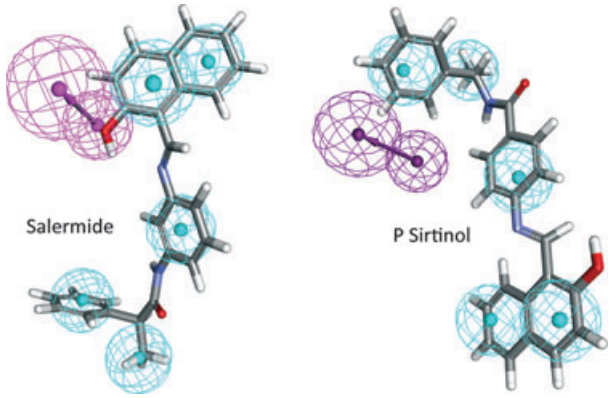

Figure 8: Dynamic pharmacophore aligned to test set. Pharmacophore features are color-coded (Hy-Hydrophobic, Cyan; HBD-Hydrogen Bond Donor, Magenta).

Table 2: Statistical parameters from decoy set

No.	Parameters	Values
1	Total number of molecules in database (D)	2000
2	Total number of actives in database (A)	15
3	Total number of hit molecules from the database (H_t)	20
4	Total number of active molecules in hit list (H_a)	13
5	%yield of actives [$(H_a/H_t) \times 100$]	65
6	%ratio of actives [$(H_a/A) \times 100$]	86.67
7	Enrichment factor[a] (EF)	0.87
8	False negatives [$A - H_a$]	2
9	False positives [$H_t - H_a$]	7
10	Goodness of hit score[b] (GH)	0.70

[a][$((H\_a/H\_t)/(A/D))/100$)].
[b][$(H_a/4H_tA)(3A + H\_t) \times (1 - ((H_t - H\_a)/(D - A))$].

we suggested that dynamics hypothesis might act as a good query to select or discriminate the potent SIRT2 inhibitors.

Virtual screening

The validated dynamics pharmacophore model was used to screen the ChemDiv chemical database to discover the novel/potent SIRT2 inhibitors. CHEMDIV consists of 0.7 million compounds; among these, 29 894 compounds satisfied the chemical features and 3D spatial arrangements of dynamic pharmacophore. Further, these molecules were sorted to 2540 by applying the maximum fit value of 4 (62). ADMET (absorption, distribution, metabolism, excretion, and toxicity) properties were calculated using ADMET module from DS, such as human intestinal absorption, aqueous solubility, blood–brain barrier (BBB), hepatotoxicity, and CYPP450 2D6 inhibition. Of these parameters, absorption, solubility and BBB play a major role in the drug-like properties. Hence, the levels of 3, 3, and 0 selected for BBB, solubility, and absorption, respectively, are applied for candidate molecules to move to a next stage in the drug discovery process. Totally, 1190 unique compounds were obtained by ADMET and tested for drug-like property by applying the Lipinski's rule of 5 (from DS) to check whether the hit molecules can be a good lead/inhibitor for SIRT2. Lipinski's rule of five states that clogP ≤ 5, molecular weight ≤ 500, and number of HBA ≤ 10 and donors ≤5. Compounds violating more than one of these rules may have problems with bioavailability; hence, these parameters were calculated by DS to eliminate the compounds that are not able to possess physicochemical properties (63). Finally, 1089 compounds have good drug-like properties that were tested by applying ADMET properties and Lipinski's rule of 5. Based on the above criteria, 1089 hits were selected for molecular docking studies which could be potent leads/inhibitors for SIRT2.

Molecular Docking study for refining the virtual screening hits

Molecular docking study (64) was performed to characterize the binding and interaction properties of ligands in C-site. The frame that shows a closest RMSD to the average structure from MD simulation was used as a representative structure. The representative structure was selected as a receptor to dock the hit compounds in SIRT2 active site.

Herein, *LigandFit* (51) and *GOLD* (65,66) were used to find whether the hits can bind in the suitable binding pocket or not. The 20 known SIRT2 inhibitors with different activity values and 1089 retrieved hits from ChemDiv database were subjected to molecular docking studies.

LigandFit

Molecular docking is a computational technique that samples conformations of small compound in protein-binding site; scoring func-

tions are used to assess which of these conformations were best complements to the protein-binding site (42). Molecular docking programs consist of two essential parts: an algorithm that searches the conformational, rotational, and translational space available to candidate molecules within binding site and an objective function to be minimized during the process. All the selected hit compounds and known inhibitors (20) with different activity values were docked into SIRT2 NAD^+ binding site to confirm the suitable binding orientation of the ligands and also to ensure its geometric fit within the active site. Flexible docking followed by consensus scoring method was performed to identify a suitable orientation of ligands in SIRT2 NAD^+ binding site. LigScore1, LigScore2, Piecewise Linear Potential 1 (PLP1), Piecewise Linear Potential 2 (PLP2), potential of mean force (PMF), Jain, Ludi1, Ludi2, Ludi3, and dock score were used for the detection of SIRT2 inhibitors. PLP scores were calculated based on the descriptions of hydrogen bond formation. PMF scores were calculated by summing pairwise interaction terms over all interatomic pairs of the receptor–ligand complex. Dock score was considered as the degree of difficulty about ligand moving into the binding site. Jain and Ludi scores were consulted in hydrophobic interaction and degree of freedom, respectively.

Before analyzing the docking result of the hit leads, docking procedure was validated using the known SIRT2 inhibitors. In the interpretation of docked-known inhibitors, based on consensus scoring function, Jain and LUDI scoring functions were able to retrieve reasonable pose of the most of the active molecules (Table 3). It was reported that the potent SIRT2 inhibitors should form a hydrogen bond interactions with critical residues (Q167, N168, I169, and D170) present in the B- and C-sites of NAD^+ binding pocket (43,67,68). Hence, these interactions were manually checked for the known compounds selected based on the Jain and LUDI scoring functions. Most of the active molecules had shown good hydrogen bond interactions with the critical residues such as Q167, N168, I169, and D170 as well as the necessary hydrophobic interactions with the hydrophobic residues of the putative SIRT2 active site. Most of the low and inactive compounds failed to form hydrogen bond interactions with the B- and C-site residues.

Hence, the same analysis procedure has been performed to select the potent leads from the hit molecules derived from a virtual screening process. Based on the Jain and LUDI scores, 111 was selected as a best lead to inhibit SIRT2. To sort out these molecules, visual inspection of the docked hit compounds was carried out to find the critical hydrogen bond interactions of hits with SIRT2. Most of the sorted molecules, using Jain and LUDI score, show good interactions with the critical residues such as Q167, N168, I169, and D170. The main aim of this visualization process is to eliminate the molecules that are not able to show the hydrogen bond interactions with the critical residues present in SIRT2 NAD^+ binding site. Based on the hydrogen bond analysis, 89 hits were selected as a potent leads for SIRT2.

GOLD

The ligand binding site was defined as a collection of atoms enclosed within a sphere of 10 Å radius around the carboxyl position of Q167. To validate the binding site, initially we docked the few known inhibitors of SIRT2. Most of the well-known inhibitors show the fitness score >50, and also all the compounds have good interactions with the most of the critical amino acids present in B- and C-sites of NAD^+ binding pocket (Table 3). Therefore, the *GOLD* fitness score of greater than 50 was taken as a cut-off range to sort out the screened hit molecules from the databases. Only 21 compounds have *GOLD* fitness score greater than 50, and it was manually checked for the critical hydrogen bond interactions. Inter-

Table 3: Score values for 20 known inhibitors of SIRT2

Name	Chemical formula	IC_{50} nM	Dock score	Jain	Ludi1	Ludi2	Ludi3	Gold Score	Aff[a]	PMF	PLP1	PLP2	Ligscore1	Ligscore2
Salermide	$C_{26}H_{22}N_2O_2$	0.41	96.70	4.87	677	570	603	62.17	−8.5	56.49	94.74	95.52	3.94	5.81
Comp1	$C_{55}H_{46}Cl_2N_6O_5$	0.59	113.69	4.96	996	728	850	62.17	−7.9	139.09	130.06	122.07	4.22	7.69
Comp2	$C_{20}H_{14}BrO_2$	1	74.79	3.72	397	404	441	62.00	−8.1	48.79	71.06	67.71	1.8	4.95
Suramin	$C_{55}H_{48}N_6O_5$	1.15	112.73	1.68	658	567	694	63.88	−8.8	172.06	111.9	100.91	2.5	3.4
Comp3	$C_{55}H_{48}N_6O_5$	1.2	112.73	1.67	658	567	694	66.77	−8.4	172.27	111.91	100.91	2.4	4.1
Comp4	$C_{57}H_{52}N_6O_5$	1.2	118.41	2.81	736	571	708	59.33	−10.3	126.45	108.37	102.86	3.1	5.4
NF675	$C_{48}H_{43}N_5O_4$	2.26	105.11	1.57	644	484	619	55.78	−10.5	126	101.42	91.55	3.39	6.7
Comp5	$C_{14}H_{15}ClN_2O$	2.77	88.03	2.7	260	264	379	53.46	−8.5	51.42	53.95	52.12	1.25	4.02
Comp6	$C_{13}H_{13}ClN_2O$	4	77.65	1.12	275	287	404	33.89	−7.6	36.68	42.82	40.53	1.09	3.84
Comp7	$C_{19}H_{13}BrO_2$	5.2	76.14	4.2	423	397	449	31.52	−8	69.62	81.15	79.4	2.96	5.1
Comp8	$C_{14}H_{16}N_2O$	6	70.37	1.25	231	235	238	35.95	−8.5	46.89	46.75	42.79	1.17	3.9
Comp9	$C_{20}H_{16}N_2O2$	14	82.63	2.25	556	456	493	34.73	−8.9	49.38	67.45	65.89	2.69	5
Ex527	$C_{13}H_{12}N_2O$	19	64.03	1.91	363	298	267	38.43	−8.5	16.53	55.88	48.53	2.98	4.46
p-sirtinol	$C_{26}H_{22}N_2O2$	26	52.25	1.41	229	222	309	37.66	−8.7	27.84	47.11	44.2	1.9	3.93
B2	$C_{21}H_{21}ClN_3O_3$	35	88.07	7.34	748	628	610	32.63	−7.7	54.01	101.28	96.66	2.17	5.42
Sirtinol	$C_{26}H_{22}N_2O2$	38	93.11	4.54	469	433	530	35.95	−7.3	65.43	89.73	79.65	3.31	5.24
Cambinol	**$C_{21}H_{16}N_2O_2S$**	59	73.34	3.34	542	489	545	34.12	−7.2	68.85	73.97	72.47	3.04	4.82
Comp10	**$C_{26}H_{22}N_2O_2$**	74	97.78	5.31	721	580	764	33.09	−7.5	81.17	99.29	96.52	3.33	5.89
Tripos 354328	$C_{18}H_{14}N_2O4$	136	83.83	3.09	512	449	509	35.06	−6.2	66.82	71.14	70.47	3.03	4.86
Tripos 551502	$C_{13}H_{14}N_2O$	200	53.05	3.24	361	330	348	29.50	−5.2	36.33	55.82	52.69	3.15	4.46

[a]Binding affinity.

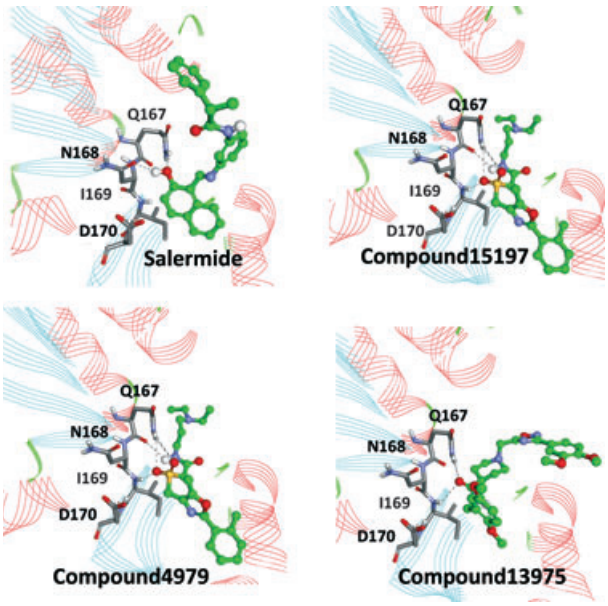

Figure 9: Docking conformation of the hit molecules from virtual screening.

estingly, all the compounds showed a good hydrogen bond interactions with Q167, N168, I169, and D170 (Figure 9).

Comparing the results of *LigandFit* and *GOLD* docking, 21 compounds from the database showed a good hydrogen bond interactions with the important amino acids such as Q167, N168, I169, and D170, and also all the molecules have good score (Jain and LUDI scores/*LigandFit* and Gold fitness score/*GOLD*) values (Table 4). Hence, these 21 molecules were selected to find the binding affinity with SIRT2 using VINA from AUTODOCK. Binding affinity was calculated to suggest how well the interactions formed between the small molecules and important residues in the active site of protein. To cross-check the ability of calculating binding affinity in VINA, 20 known inhibitors were analyzed first. The known inhibitors had shown a good correlation between the activity values and the binding affinity (Table 3). The *X*, *Y*, and *Z* co-ordinates of the 20 known inhibitors of SIRT2 and the 21 hit leads are shown in Tables S1 and S2. Hence, we calculated the binding affinity for the 21 hit compounds, and the result is shown in Table 4. All the hit compounds had shown a good binding affinity near to the reported inhibitors. Furthermore, the selected leads satisfied the demands of a dynamic hypothesis. From the above results, it has been shown that the screened molecules can effectively disrupt the SIRT2 active site and satisfied the structural requirement of a new type of SIRT2 inhibitors. Hence, we suggest these 21 molecules (Figure 10) for the medicinal chemists who are interested to work in SIRT2 inhibitors.

Conclusions

SIRT2, one of the emerging targets in chemogenomic approach, is a NAD^+-dependent deacetylation protein. The complex structure was prepared by docking sirtinol in C-site of NAD^+ binding pocket using apo-form of SIRT2 as a receptor. The resultant sirtuin2 complex and apo-form were subjected into 5-nseconds MD simulation to find a suitable position of sirtinol in NAD^+ binding pocket. The three representative structures from MD simulation were selected based on cluster analyses, and these structures were subjected to generate the receptor-based pharmacophore using LigandScout. The three generated structure-based hypothesis was merged to produce a

Table 4: Score values for 21 potent leads from databases and the known inhibitors

Compound	Chemical formula	Dock score	Jain	Ludi1	Ludi2	Ludi3	Gold Score	Aff[a]	PMF	PLP1	PLP2	Ligscore1	Ligscore2
11315	$C_{21}H_{26}ClN_3O_6S$	98.58	4.04	617	514	598	51.22	−7.5	62.85	92.25	89.09	3.5	5.22
12381	$C_{25}H_{30}N_2O6$	103.63	4.22	509	476	469	56.39	−7.9	82.53	91.69	84.08	3.16	5.76
13954	$C_{25}H_{30}N_4O6$	103.78	2.85	505	431	521	53	−8.4	91.67	93.87	81.83	2.85	5.43
14831	$C_{23}H_{34}N_4O_4S_2$	102.59	4.73	451	469	549	70.01	−8	82.8	100.01	92.03	2.39	5.35
15197	$C_{22}H_{27}N_3O_5S$	101.67	2.77	465	413	567	51.26	−8.3	95.2	95.56	86.19	3.9	6.2
185	$C_{21}H_{25}N_3O_4$	91.22	6.29	977	572	495	50.42	−8	49.59	92.34	89.83	2.78	5.01
2092	$C_{23}H_{26}ClN_3O_4S$	94.68	4.18	536	465	380	52.74	−8.8	58.61	91.25	82.01	2.16	5.39
2969	$C_{20}H_{28}N4O_3S$	94.41	5.01	491	469	534	51.45	−8.7	72.36	95.68	90.45	3.81	5.7
3775	$C_{23}H_{31}N_3O_5S$	102.36	5.17	495	447	433	55.66	−8.9	100.03	85.17	79.44	3.56	5.36
4582	$C_{23}H_{31}N_5O_4S$	96.88	5.82	509	491	528	51.52	−8.7	76.36	90.55	88.36	3.68	4.9
4653	$C_{18}H_{21}F_2N_3O_5S$	100.03	4.25	512	462	434	53.93	−8.3	75.63	100.32	97.03	3.3	5.05
4657	$C_{18}H_{22}ClN_3O_5S$	93.17	4.44	544	489	461	53.89	−7.8	53.45	89.83	81.75	4.41	5.72
4660	$C_{19}H_{25}N_3O_5S$	100.67	5.38	518	472	448	50.42	−8.4	66.51	102.63	98.76	3.08	5.26
4770	$C_{22}H_{24}N_2O_4S$	98.26	5.46	571	512	653	50.7	−8.1	73.73	97.95	97.88	2.68	5.1
4979	$C_{21}H_{31}N_3O_4S$	102.51	4.69	486	446	412	54.5	−7.3	82.53	90.56	88.82	2.65	4.96
4982	$C_{22}H_{24}N_2O_5S$	97.97	2.94	369	345	357	55.5	−8.7	79.29	88.28	81.7	3.93	5.82
4988	$C_{19}H_{26}N_2O_4S$	98.26	6.75	535	485	506	53.27	−7.5	74.14	96.25	92.95	2.92	5.15
4992	$C_{22}H_{24}N_2O_5S$	108.39	5.5	528	462	497	62.1	−7.8	87.08	98.39	92.09	3.21	4.92
5099	$C_{24}H_{31}N_3O_5S$	97.97	4.55	444	413	558	50.41	−7.8	82.07	103.34	96.74	3.26	5.3
7217	$C_{23}H_{33}N_3O_5S$	94.12	4.99	502	458	404	63	−7.6	77.97	106.39	99.57	4.07	6.09
9978	$C_{25}H_{32}N_4O_4S$	104.34	4.92	360	402	366	53.18	−7.6	46.44	95.51	89.27	1.88	5.13

[a]Binding affinity.

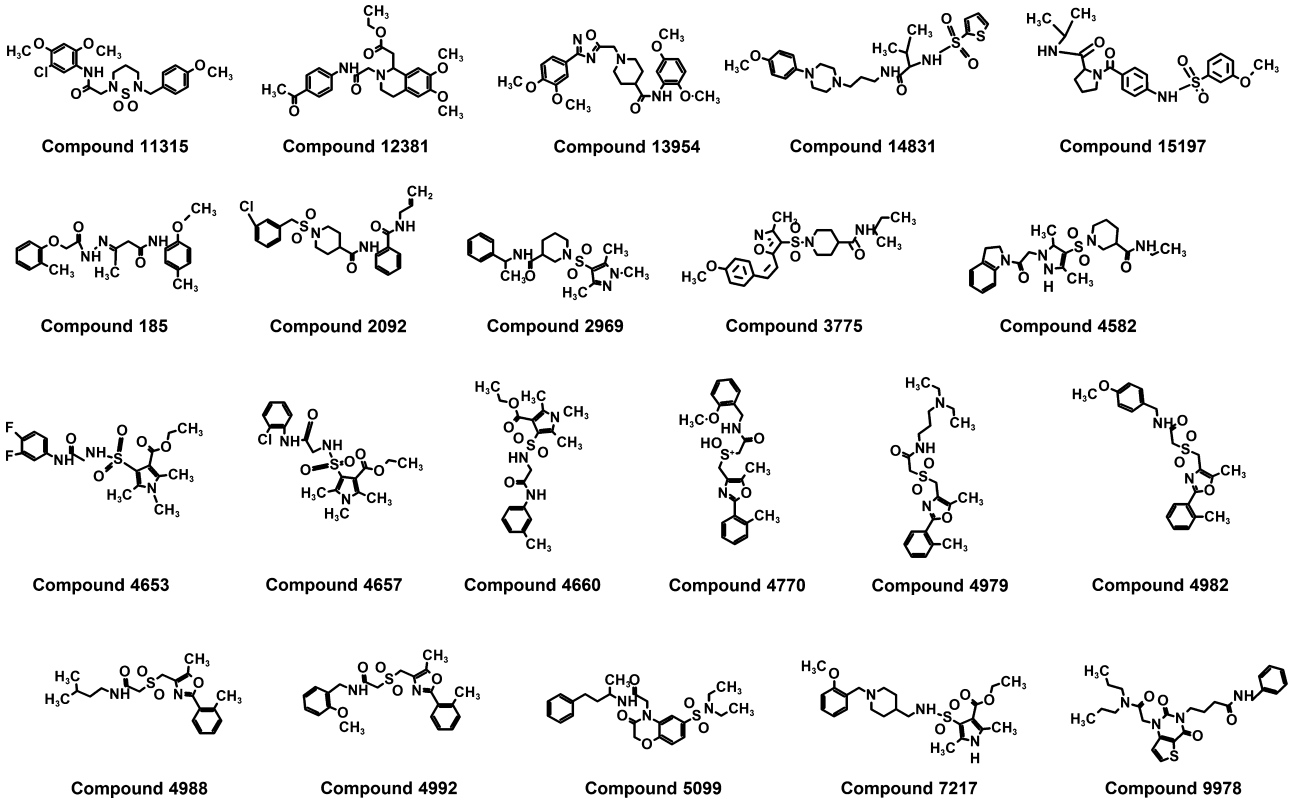

Figure 10: 2D structure of the final 21 hit compounds.

dynamic hypothesis that was validated by test and decoy sets. The results of test and decoy sets revealed that the dynamic hypothesis can differentiate the active from low active SIRT2 inhibitors. Hence, dynamic hypothesis was used a query to screen the ChemDiv database; as a result, 1089 molecules satisfied all chemical features present in dynamics hypothesis as well as passed the ADMET filtration and drug-like properties. Molecular docking (*LigandFit* and *GOLD*) was used to find a suitable orientation of the filtered leads in the C-site of NAD^+ binding pocket. Finally, 21 leads were selected as potent inhibitors for SIRT2 based on the consensus scoring valued from LigandFit, Gold fitness score, and the binding affinity. From the above results, we confirmed that the chemical features present in dynamics hypothesis are complement to SIRT2 active site. This methodology of analyzing the dynamic motion of the protein, then developing dynamic receptor–based pharmacophore model to retrieve hits, and finally performing docking into plausible conformations would be a reliable procedure to apply in identifying new lead molecules.

Acknowledgments

This research was supported by Basic Science Research Program (2009-0073267), Pioneer Research Center Program (2009-0081539), and Management of Climate change Program (2010-0029084) through that National Research Foundation of Korea (NRF) funded by the Ministry of Education, Science and Technology (MEST) of Republic of Korea. And this work was also supported by the Next-Generation BioGreen21 Program (PJ008038) from Rural Development Administration (RDA) of Republic of Korea.

References

1. Wolffe A.P., Matzke M.A. (1999) Epigenetics: regulation through repression. Science;286:481–486.
2. Biel M., Wascholowski V., Giannis A. (2005) Epigenetics – an Epicenter of gene regulation: histones and histone-modifying enzymes. Angew Chem Int Ed;44:3186–3216.
3. Schäfer S., Jung M. (2005) Chromatin modifications as targets for new anticancer drugs. Arch Pharm;338:347–357.
4. Jenuwein T., Allis C.D. (2001) Translating the histone code. Science;293:1074–1080.
5. Santos-Rosa H., Caldas C. (2005) Chromatin modifier enzymes, the histone code and cancer. Eur J Cancer;41:2381–2402.
6. Yang X.-J., Seto E. (2008) The Rpd3/Hda1 family of lysine deacetylases: from bacteria and yeast to mice and men. Nat Rev Mol Cell Biol;9:206–218.
7. Lehrmann H., Pritchard L.L., Harel-Bellan A. (2002) A Histone acetyltransferases and deacetylases in the control of cell proliferation and differentiation. Adv Cancer Res;86:41–65.
8. Marks P.A., Breslow R. (2007) Dimethyl sulfoxide to vorinostat: development of this histone deacetylase inhibitor as an anticancer drug. Nat Biotech;25:84–90.

9. Richon V.M., Garcia-Vargas J., Hardwick J.S. (2009) Development of vorinostat: current applications and future perspectives for cancer therapy. Cancer Lett;280:201–210.
10. Sakkiah S., Baek A., Lee K.W. (2012) Pharmacophore modeling and molecular dynamics simulation to identify the critical chemical features against human Sirtuin2 inhibitors. J Mol Struct;1011:66–75.
11. Brain J.N., Eric V. (2004) Sirtuins: Sir2-related NAD-dependent protein deacetylases. Genome Biol;5:224–224.12.
12. Schemies J., Sippl W., Jung M. (2009) Histone deacetylase inhibitors that target tubulin. Cancer Lett;280:222–232.
13. Sauve A.S., Wolberger C., Schramm V.L., Boeke J.D. (2006) The biochemistry of sirtuins. Annu Rev Biochem;75:435–465.
14. Brachmann C.B., Sherman J.M., Devine S.E., Cameron E.E., Pillus L., Boeke J.D. (1995) The SIR2 gene family, conserved from bacteria to humans, functions in silencing, cell cycle progression, and chromosome stability. Genes Dev;9:2888–2902.
15. Guarente L. (2000) Sir2 links chromatin silencing, metabolism, and aging. Genes Dev;14:1021–1026.
16. Lin S.j., Ford E., Haigis M., Liszt G., Guarente L. (2004) Calorie restriction extends yeast life span by lowering the level of NADH. Genes Dev;18:12–16.
17. Vaquero A., Scher M.B., Lee D.H., Sutton A., Cheng H.-L., Alt F.W., Serrano L., Sternglanz R., Reinberg D. (2006) SirT2 is a histone deacetylase with preference for histone H4 Lys 16 during mitosis. Genes Dev;20:1256–1261.
18. Bellamacina C.R. (1996) The nicotinamide dinucleotide binding motif: a comparison of nucleotide binding proteins. FASEB J;10:1257–1269.
19. Finnin M.S., Donigian J.R., Pavletich N.P. (2001) Structure of the histone deacetylase SIRT2. Nat Struct Mol Biol;8:621–625.
20. Sauve A.A., Schramm V.L. (2003) Sir2 regulation by nicotinamide results from switching between base exchange and deacetylation chemistry. Biochemistry;42:9249–9256.
21. Chang J.H., Kim H.C., Hwang K.Y., Lee J.W., Jackson S.P., Bell S.D., Cho Y. (2002) Structural basis for the NAD-dependent deacetylase mechanism of sir2. J Biol Chem;277:34489–34498.
22. Borra M.T., Langer M.R., Slama J.T., Denu J.M. (2004) Substrate specificity and kinetic mechanism of the Sir2 family of NAD+-dependent histone/protein deacetylases. Biochemistry;43:9877–9887.
23. Grubisha O., Rafty L.A., Takanishi C.L., Xu X., Tong L., Perraud A.L., Scharenberg A.M., Denu J.M. (2006) Metabolite of SIR2 reaction modulates TRPM2 ion channel. J Biol Chem;28:14057–14065.
24. Heltweg B., Gatbonton T., Schuler A.D., Posakony J., Li H., Goehle S., Kollipara R., DePinho R.A., Gu Y., Simon J.A., Bedalov A. (2006) Antitumor activity of a small-molecule inhibitor of human silent information regulator 2 enzymes. Cancer Res;66:4368–4377.
25. Guarente L., Picard F. (2005) Calorie Restriction – the SIR2 Connection. Cell;120:473–482.
26. Picard F., Kurtev M., Chung N., Topark-Ngarm A., Senawong T., Machado de Oliveira R., Leid M., Michael W., Guarente L. (2004) Sirt1 promotes fat mobilization in white adipocytes by repressing PPAR-[gamma]. Nature;429:771–776.
27. Tang B.L. (2005) Alzheimer's disease: channeling APP to non-amyloidogenic processing. Biochem Biophys Res Commun;331:375–378.
28. Huhtiniemi T., Suuronen T., Rinne V.M., Wittekindt C., Lahtela-Kakkonen M., Jarho E., Wallen E.A., Salminen A., Poso A., Leppanen J. (2008) Oxadiazole-carbonylaminothioureas as SIRT1 and SIRT2 inhibitors. J Med Chem;51:4377–4380.
29. North B.J., Marshall B.L., Borra M.T., Denu J.M., Verdin E. (2003) The Human Sir2 Ortholog, SIRT2, Is an NAD+-Dependent Tubulin Deacetylase. Mol Cell;11:437–444.
30. Hubbert C., Guardiola A., Shao R., Kawaguchi Y., Ito A., Nixon A., Yoshida M., Wang X.F., Yao T.P. (2002) HDAC6 is a microtubule-associated deacetylase. Nature;417:455–458.
31. Kiviranta P.H., Salo H.S., Leppanen J., Rinne V.M., Kyrylenko S., Kuusisto E., Suuronen T., Salminen A., Poso A., Lahtela-kakkonen M., Wallen E.A. (2008) Characterization of the binding properties of SIRT2 inhibitors with a N-(3-phenylpropenoyl)-glycine tryptamide backbone. Bioorg Med Chem;16:8054–8062.
32. Hiratsuka M., Inoue T., Toda T., Kimura N., Shirayoshi Y., Kamitani H., Watanabe T., Ohama E., Tahimic C.G., Kurimasa A., Oshimura M. (2003) Proteomics-based identification of differentially expressed genes in human gliomas: down-regulation of SIRT2 gene. Biochem Biophys Res Commun;309:558–566.
33. Outeiro T.F., Kontopoulos E., Altmann S.M., Kufareva I., Strathearn K.E., Amore A.M., Volk C.B., Maxwell M.M., Rochet J.C., McKLean P.J., Young A.B., Abagyan R., Feany M.B., Hyman B.T., Kazantsev A.G. (2007) Sirtuin 2 inhibitors rescue alpha-synuclein-mediated toxicity in models of Parkinson's disease. Science;317:516–519.
34. Inoue T., Hiratsuka M., Osaki M., Yamada H., Kishimoto I., Yamaguchi S., Nakano S., Katoh M., Ito H., Oshimura M. (2006) SIRT2, a tubulin deacetylase, acts to block the entry to chromosome condensation in response to mitotic stress. Oncogene;26:945–957.
35. Dryden S., Nahhas F.A., Nowak J.E., Goustin A.-S., Tainsky M.A. (2003) Role for human SIRT2 NAD-dependent deacetylase activity in control of mitotic exit in the cell cycle. Mol Cell Biol;23:3173–3185.
36. Bae N.S., Swanson M., Vassilev A., Howard B.H. (2004) Human histone deacetylase SIRT2 interacts with the homeobox transcription factor HOXA10. J Biochem;135:695–700.
37. Wang F., Nguyen M., Qin F.X.-F., Tong Q. (2007) SIRT2 deacetylates FOXO3a in response to oxidative stress and caloric restriction. Aging Cell;6:505–514.
38. Matsushita N., Takami Y., Kimura M., Tachiiri S., Ishiai M., Nakayama T., Takata M. (2005) Role of NAD-dependent deacetylases SIRT1 and SIRT2 in radiation and cisplatin-induced cell death in vertebrate cells. Genes Cells;10:321–332.
39. Luo J., Nikolaev A.Y., Imai S., Chen D., Su F., Shiloh A., Guarente L., Gu W. (2001) Negative control of p53 by Sir2alpha promotes ce;; survival under stress. Cell;107:137–148.
40. Cohen H.Y., Lavu S., Bitterman K.J., Hekking B., Imahiyerobo T.A., Imahiyerobo T.A., Miller C., Frye R., Ploegh H., Kessler B.M., Sinclaie D.A. (2004) Acetylation of the C terminus of Ku70 by CBP and PCAF controls Bax-mediated apoptosis. Mol Cell;13:627–638.

41. Smellie A., Teig S. L., Towbin P. (1995) Poling: Promoting conformational variation. Journal of Computational Chemistry; 16:171–187.
42. Sakkiah S., Thangapandian S., John S., Lee K.W. (2011) Pharmacophore based virtual screening, molecular docking studies to design potent heat shock protein 90 inhibitors. Eur J Med Chem;46:2937–2947.
43. Medda F., Russell R.J.M., Higgins M., McCarthy A.R., Campbell J., Slawin A.M.Z., David P.L., Lain S., Westwood N.J. (2009) Novel cambinol analogs as sirtuin inhibitors: synthesis, biological evaluation, and rationalization of activity. J Med Chem;52:2673–2682.
44. Tervo A.J., Kyrylenko S., Niskanen P., Salminen A., Leppänen J., Nyrönen T.H., Jarvinen T., Poso A. (2004) An in silico approach to discovering novel inhibitors of human sirtuin Type 2. J Med Chem;47:6292–6298.
45. Lindahl E., Hess B., van der Spoel D. (2001) GROMACS 3.0: a package for molecular simulation and trajectory analysis. J Mol Model;7:306–317.
46. Berendsen H.J.C., van der Spoel D., van Drunen R. (1995) GROMACS: a message-passing parallel molecular dynamics implementation. Comput Phys Commun;91:43–56.
47. Van Der Spoel D., Lindahl E., Hess B., Groenhof G., Mark A.E., Berendsen H.J.C. (2005) GROMACS: fast, flexible, and free. J Comput Chem;26:1701–1718.
48. Wolber G., Dornhofer A., Langer T. (2006) Efficient overlay of small organic molecules using 3D pharmacophores. J Comput Aided Mol Des;20:773–788.
49. Barreca M.L., De Luca L., Iraci N., Rao A., Ferro S., Maga G., Chimirri A. (2007) Structure-based pharmacophore identification of new chemical scaffolds as non-nucleoside reverse transcriptase inhibitors. J Chem Inf Model;47:557–562.
50. Jones G., Willett P., Glen R. (1995) Molecular recognition of receptor sites using a genetic algorithm with a description of desolvation. J Mol Biol;245:43–53.
51. Venkatachalam C.M., Jiang X., Oldfield T., Waldman M. (2003) LigandFit: a novel method for the shape-directed rapid docking of ligands to protein active sites. J Mol Graph Model;21:289–307.
52. Brooks B., Bruccoleri R., Olafson B., States D., Swaminathan S., Karplus M. (1983) CHARMM: a program for macromolecular energy, minimization, and dynamics calculations. J Comput Chem;4:187–217.
53. Smellie A., Teig S.L., Towbin P. (1995) Poling: promoting conformational variation. J Comput Chem;16:171–187.
54. Schuttelkopf A.W., Aalten D.M.V. (2004) PRODRG: a tool for high-throughput crystallography of protein-ligand complexes. Acta Crystallogr D Biol Crystallogr;60:1355–1363.
55. Berendsen H.J.C., Postma J.P.M., van Gunsteren W.F., Hermans J. (1981) Interaction models for water in relation to protein hydration. Intermolecular Forces;33:1–342.
56. Hess B., Bekker H., Berendsen H.J.C., Fraaije J.G.E.M. (1997) LINCS: a linear constraint solver for molecular simulations. J Comput Chem;18:1463–1472.
57. Miyamoto S., Kollman P. (1992) Settle: an analytical version of the SHAKE and RATTLE algorithm for rigid water models. J Comput Chem;13:952–962.
58. Berendsen H.J.C., Postma J.P.M., van Gunsteren W.F., DiNola A., Haak J.R. (1984) Molecular dynamics with coupling to an external bath. J Chem Phys;81:3684–3690.
59. Wolber G., Langer T. (2005) LigandScout:3D pharmacophores derived from protein-bound ligands and their use as virtual screening fliters. J Chem Inf Model;45:160–169.
60. Avalos J.L., Bever K.M., Wolberger C. (2005) Mechanism of sirtuin inhibition by nicotinamide: altering the NAD+ cosubstrate specificity of a Sir2 enzyme. Mol Cell;17:855–868.
61. Zhao K., Harshaw R., Chai X., Marmorstein R. (2004) Structural basis for nicotinamide cleavage and ADP-ribose transfer by NAD(+)-dependent Sir2 histone/protein deacetylases. Proc Nat Acad Sci USA; 101:8563–8568.
62. Sakkiah S., Krishnamoorthy N., Gajendrarao P., Thangapandian S., Lee Y., Kim S., Suh J.K., Kim H.H., Lee K.W. (2009) Pharmacophore mapping and virtual screening for SIRT1 activators. Bull Korean Chem Soc;30:1152–1156.
63. Sakkiah S., Thangapandian S., John S., Kwon Y.J., Lee K.W. (2010) 3D QSAR pharmacophore based virtual screening and molecular docking for identification of potential HSP90 inhibitors. Eur J Med Chem;45:2132–2140.
64. Sakkiah S., Thangapandian S., John S., Lee K.W. (2011) Identification of critical chemical features for Aurora kinase-B inhibitors using Hip-Hop, virtual screening and molecular docking. J Mol Struct;985:14–26.
65. Hartshorn M.J., Verdonk M.L., Chessari G., Brewerton S.C., Mooij W.T.M., Mortenson P.N., Murray C.W. (2007) Diverse, high-quality test set for the validation of protein–ligand docking performance. J Med Chem;50:726–741.
66. Verdonk M.L., Chessari G., Cole J.C., Hartshorn M.J., Murray C.W., Nissink J.W., Taylor R.D., Taylor R. (2005) Modeling water molecules in protein–ligand docking using GOLD. J Med Chem;48:6504–6515.
67. Lin S.-J., Guarente L. (2003) Nicotinamide adenine dinucleotide, a metabolic regulator of transcription, longevity and disease. Curr Opin Cell Biol;15:241–246.
68. Kiviranta P.H., Leppänen J., Rinne V.M., Suuronen T., Kyrylenko O., Kyrylenko S., Kuusisto E., Tervo A.J., Jarvinen T., Salminen A., Poso A., Wallen E.A. (2007) N-(3-(4-Hydroxyphenyl)-propenoyl)-amino acid tryptamides as SIRT2 inhibitors. Bioorg Med Chem Lett;17:2448–2451.

Supporting Information

Additional Supporting Information may be found in the online version of this article:

Table S1. The X, Y, Z co-ordination of the 20 known SIRT2 inhibitors.

Table S2. The X, Y, Z co-ordination of the 21 hit compounds from the databases.

Please note: Wiley-Blackwell is not responsible for the content or functionality of any supporting materials supplied by the authors. Any queries (other than missing material) should be directed to the corresponding author for the article.